Labeling of Hyaluronic Acids with a Rhenium-Tricarbonyl Tag and Percutaneous Penetration Studied by Multimodal Imaging

Lucas Henry, Nicolas Delsuc, Cécile Laugel, François Lambert, Christophe Sandt, Sarah Hostachy, Anne-Sophie Bernard, Hélène Bertrand, Laurence Grimaud, Arlette Baillet-Guffroy, et al.

Labeling of Hyaluronic Acids with a Rhenium-tricarbonyl Tag and Percutaneous Penetration Studied by Multimodal Imaging

Lucas Henry,[‡] Nicolas Delsuc,[‡] Cécile Laugel,[§] François Lambert,[‡] Christophe Sandt,[∥] Sarah Hostachy,[‡] Anne-Sophie Bernard,[‡] Hélène C. Bertrand,[‡] Laurence Grimaud,[⊥] Arlette Baillet-Guffroy,[§] and Clotilde Policar*[,‡]

[‡]Laboratoire des biomolécules, LBM, Département de chimie, École normale supérieure, PSL University, Sorbonne Université, CNRS, 75005 Paris, France

[§]Laboratory of Analytical Chemistry, Lip(Sys)2, (EA 7357), Faculty of Pharmacy, Paris-Sud, University of Paris-Saclay, 5 Rue Jean-Baptiste Clément, 92296 Chatenay-Malabry, France

[∥]SMIS beamline, Synchrotron SOLEIL Saint-Aubin, 91192 Gif-sur-Yvette Cedex, France

[⊥]PASTEUR, Département de chimie, École normale supérieure, PSL Research University, Sorbonne Universités, UPMC Univ. Paris 06, CNRS, 75005 Paris, France

ABSTRACT: Hyaluronic acids were labeled with a rhenium-tricarbonyl used as single core multimodal probe for imaging and their penetration into human skin biopsies was studied using IR microscopy and fluorescence imaging (labeled SCoMPI). The penetration was shown to be dependent on the molecular weight of the molecule and limited to the upper layer of the skin.

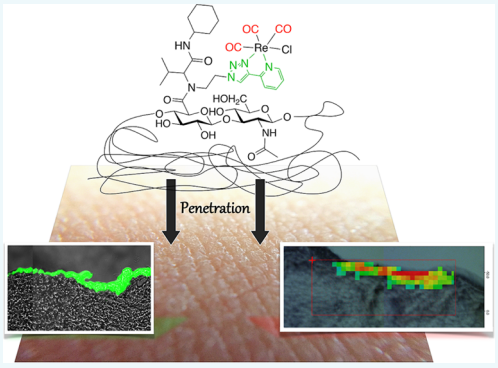

Hyaluronic acid (HA) is a polymer of disaccharides made of D-glucuronic acid and D-*N*-acetylglucosamine moieties, linked by alternating β-1,4 and β-1,3-glycosidic bonds,[1] with molecular weights (MW) up to 10^7 Da. HA is found in tissues and body fluids of almost all living organisms.[2] This highly hydrophilic molecule binds a thousand times its volume of water,[3] and is commonly used as a medicine, for instance, injected into joints to treat arthritis or in dermis to fill facial wrinkles.[4] Low MW HAs are only used to maintain hydration of epidermis after topical application, whereas high MW HAs are also used as filling agent after cutaneous injection.[3]

In order to investigate their penetration into skin, HAs of two MW have been labeled with a multimodal rhenium-tricarbonyl probe. Several $Re(CO)_3$ tags displaying a fluorescent and an IR modality on the same molecular moiety have been recently developed. These SCoMPIs—for Single Core Multimodal Probes for Imaging[5−7]—are fluorescent with an absorption in the 350 nm range and an emission in the yellow-green (around 550 nm).[6,8,9] They also show two characteristic IR-absorption bands in the transparency windows of biological tissues in the mid-IR (between 1800 and 2200 cm^{-1}), namely, E and A_1 for the antisymmetric and symmetric CO-stretching vibrations, respectively.[7,10,11] Metal-carbonyls have already been characterized and used as organelle trackers[5,12−14] or for the labeling and imaging of molecules of biological interest,[6,7,8−17] such as amino acids and peptides,[13,16−21] peptide-nucleic acids,[22] vitamins,[23] hormones,[24] or medicines.[25] Interestingly, the A_1-band, that is a singly degenerated band, can be used for quantification purposes.[11,26−29] IR-imaging is a challenging technique. Its lateral resolution is limited to a few μm ($\lambda/2$, so about 2.5 μm at 2000 cm^{-1} or 5 μm) with an optical detection but resolution down to 20−50 nm can be obtained using near-field techniques, such as AFM-IR.[30,31] IR-imaging can be recorded not only on dedicated synchrotron beamlines (synchrotron-based FTIR spectromicroscopy or SR-FTIR-SM) but also on IR-microscopes that are commercially available with focal-plane array detectors enabling fast imaging, and this will certainly popularize FTIR-based spectromicroscopy (FTIR-SM) in biology. One interest of the SCoMPIs as IR-probes is their reliability for quantification in biological environments in which polarities have a wide range of diversity. Generally speaking, luminescence cannot be directly implemented for absolute quantification, since the quantum yield is highly dependent on

Scheme 1. Synthesis of the Graftable SCoMPI 5 and Labeling of HA Using a Ugi Condensation[a]

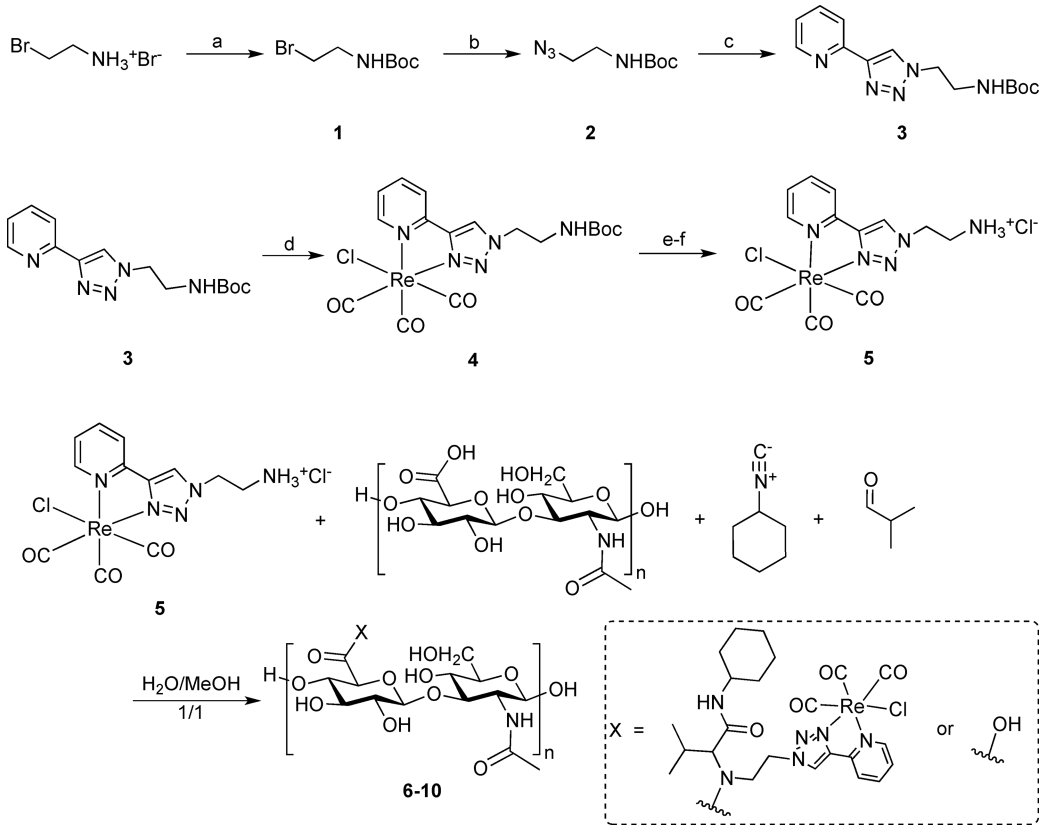

[a](a) Boc_2O, DIPEA, THF, 1 h, r.t., quantitative. (b) NaN_3, NaI, acetone/H_2O, 40 h, 35 °C, 66%. (c) 2-ethynylpyridine, $CuSO_4$, sodium ascorbate, acetone/H_2O, 3 h, r.t, 62%. (d) $Re(CO)_5Cl$, toluene, 1.5 h, 80 °C, 88%. (e) CH_2Cl_2, TFA, 1 h, 25 °C. (f) CH_3OH, HCl, 10 min, 25 °C, 95%.

Table 1. Distribution of HAs in the Skin

					distribution in the skin	
molecule	MW of HA (kDa)	labeling % (IR)[a]	labeling % (NMR)[b]	soluble in water	7 h	24 h
6	10	∼5%	∼3−4%	Yes	Not observed	Hotspots mapped by IR and fluorescence in the SC (Figure S8)
7	10	∼20%	∼20%	Yes	Hardly detectable by IR, hotspots mapped by fluorescence in the SC (Figure S9)	Homogeneously distributed in the SC and very weak amount in the VE (Figure 2, IR and fluorescence)
8	10	∼40%	-	No		
9	400−1000	∼20%	-	No		
10	400−1000	∼5%	-	Yes	Not observed	Inhomogeneous, hotspots in the SC (Figure S10)

[a]% of functionalized carboxylic acid functions determined by IR. [b]% of functionalized carboxylic acid functions determined by ^1H NMR.

the environment.[6,32,33] In contrast, the molar absorption coefficient of the A_1-band of the $Re(CO)_3$ moiety is not strongly dependent on the solvent.[6,7,29] Therefore, this band can be used for absolute titration, as previously performed.[11,19,27−29] These SCoMPIs $Re(CO)_3$ probes are thus of interest, for both IR-mapping and quantification purposes, and their grafting onto biomolecules is worth exploring.

To graft the probe onto the HA, a Ugi multicomponent condensation involving the carboxylic acid functions of HA[34] was selected for its high efficiency in water,[35,36] the most appropriate solvent for HA.[36] A graftable SCoMPI bearing an amine moiety was synthesized in five steps and was reacted with HA, as described in Scheme 1 and SI.

HAs in two ranges of MW were used (10 kDa and 400−1000 kDa), with a low or high probe to HA (probe/HA) ratio (Table 1). In order to easily monitor the reaction completion using ^1H NMR, the Ugi reaction was performed in a deuterated solvent (D_2O/CD_3OD 1/1). New signals growing in the aromatic range (7.5−9.5 ppm) were assigned to the probe grafted on HA (Figure S3, SI). When no more evolution could be seen, the tagged HAs were purified by filtration over a membrane with a 3000 MW cutoff, in order to remove low-molecular-weight reactants, and the fraction containing HA was then lyophilized.

IR-spectroscopy was used to characterize the tagging of the HAs. The number of bands of CO-stretching of M(CO)s observed in the 2000 cm^{-1} wavenumber range depends on the local symmetry, with the doubly degenerated band labeled E possibly split in the case of a low symmetry.[10] Their energy positions vary with the local environment, depending on the hydrophobicity of the environment, for instance, and splittings can be observed upon aggregation or in the solid state when there is a composite environment.[10,11] The IR-spectra of **4** and

5 have been recorded in several solvents (Figure S4 and Table S2). They show the two bands in the 2000 cm^{-1} energy range. As previously published in the case of pyridyl-triazolyle based $Re(CO)_3$, the E-band is split into a doublet due to a low symmetry.[5−7,29] As shown in Figure S4 and Table S2, the positions of the A_1 band and E bands are shifted depending on the solvent nature, with shifts of about 10 to 20 cm^{-1}. Similar shifts have already been reported, with frequencies higher in hydrophobic than in hydrophilic environment.[37] The spectra of the tagged HAs show several sets of A_1 and E bands, as exemplified with **7** in Figure 1. The presence of several sets of

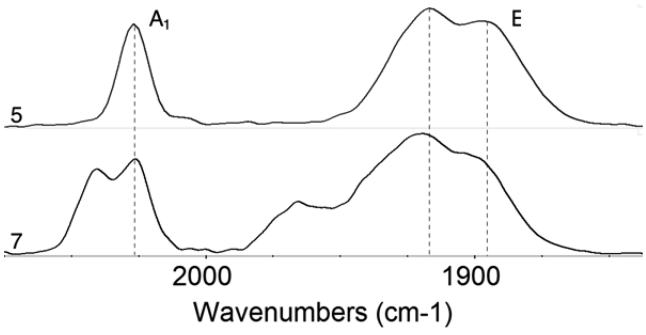

Figure 1. IR spectra obtained using ATR mode between 1820 and 2075 cm^{-1} of **5** in acetone and **7** in water (2 $mg{\cdot}mL^{-1}$). See also Figure S4 and Table S2 for the spectra of **5** in a range of solvents.

A_1 and E bands is indicative of the different local environments of the $Re(CO)_3$ moiety which can be found in a hydrophobic or hydrophilic environment depending on the fact that the SCoMPI is exposed to the solvent or buried within the polymer, where its environment may be composite and solid-state-like.

The number of grafted probes per monomeric unit (one D-glucuronic acid and one D-*N*-acetylglucosamine moiety) was evaluated by ^1H NMR when possible (compounds soluble enough: **6** and **7**) and FTIR using a calibration curve with a mixture of HA and **5** (SI). The results obtained by FTIR for the lightest compounds **6** and **7** were in good agreement with those obtained by ^1H NMR. This validates the FTIR protocol that was then applied for the heavier compounds (**8**, **9**, **10**) for which NMR quantification could not be used (see Table 1).

To investigate their ability to permeate through skin, 200 μL of a 2 $mg{\cdot}mL^{-1}$ aqueous solution of labeled HAs was applied to the surface of human skin biopsies mounted in a Franz cell chamber. After a 7- or 24-h exposure, skin samples were washed, frozen, and cut in 10-μm-thick sections that were mounted on CaF_2 windows.

The distribution of the labeled HAs in the skin was investigated using synchrotron radiation FTIR spectromicroscopy (SR-FTIR-SM, see Figure 2) or FTIR spectromicroscopy (FTIR-SM, see SI Figures S8−S10). IR spectra were recorded in the 800−4000 cm^{-1} range, and maps were generated by integrating specific bands (see SI): A_1 band (2055−2005 cm^{-1}) and CH_2 bands in the 2868−2838 cm^{-1} range. Areas with high concentration of CH_2 indicate a lipid-rich layer, corresponding to the stratum corneum (SC).[19,38] Luminescence imaging was also performed after Hoechst staining[39] to reveal cell nuclei of the viable epidermis (VE).[19]

After a 24 h exposure, **6** was hardly detectable by IR imaging but was detected by fluorescence microscopy at some spots where it accumulated (Figure S8, SI). The labeling ratio of **6**

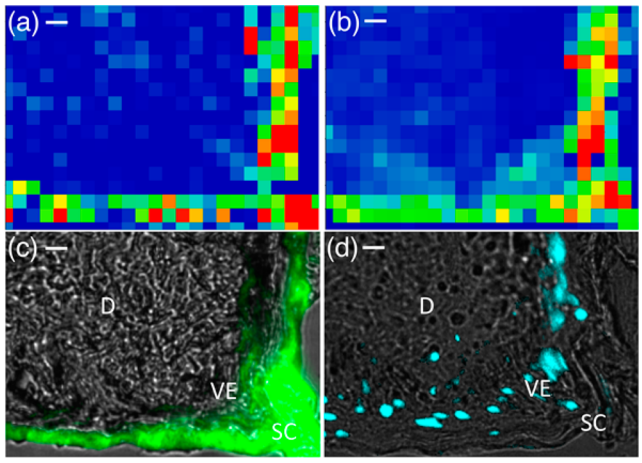

Figure 2. Map of a 10-μm-thick skin cryosection after a 24 h exposure with **7**, mounted on a CaF_2 window (scale bar = 10 μm). (a,b) SR-FTIR-SM images based on the integration of absorption bands: (a) A_1-band (2055−2005 cm^{-1}), (b) CH_2 (2868−2838 cm^{-1}), using a false color scale from blue (low) to red (high intensity), (c,d) Bright field image merged with (c) the luminescence signal of **7** (ex 350/50x, em 560/80m) and (d) nuclei staining (Hoechst, blue, ex 350/50x em 460/50m); 128 scans, 8 cm^{-1} spectral width. D = dermis, VE = viable epidermis, SC = stratum corneum.

was probably too low for an IR-detection. Compound **7**, with a labeling rate ca. four times higher, was thus investigated: its distribution after a 7 h exposure was nonhomogeneous in the skin section, with spots of high accumulation (or hotspots) and large areas showing no product (Figure S9, SI). After 24 h, an intense and homogeneous signal was observed both by IR and fluorescence and it was mainly observed in the SC. Only some weak signals were seen at few areas in the VE (Figure 2). The high MW analog with 5% tagging (**10**) was investigated and showed an inhomogeneous distribution at 24 h. Compounds **8** and **9** were not soluble enough for an epidermal application. The results are summarized in Table 1.

FTIR-SM was also used to investigate modifications of lipids and proteins of the skin in hotspots of HA after permeation of **7**. The CH_2 IR band in the 2850 cm^{-1} range assigned to lipid acyl chains is specific to the organization of lipids,[40,41] and the amide I band can be analyzed to probe a modification of the protein structure.[42] Spectra were recorded at the surface of the skin exposed to **7** for 24 h, at some points with various intensities of the A_1-band and at the surface of the skin not exposed (Figures S11 and S12, SI). No variation in peak position was seen at 2850 and 1500−1700 cm^{-1}, which suggests that **7** does not induce any modification of the organization of lipids or proteins.

In conclusion, we were able to efficiently label HAs of different MW with a $Re(CO)_3$ SCoMPI at different rates using a Ugi reaction. Their penetration into human skin biopsies was monitored using IR and fluorescence microscopies. The label percentage was an important parameter to ensure detection without modifying to an excessively large extent the physicochemical properties of the biopolymer: if too low, the compound (**6**, 10 kDa, 3−4%) was not seen, but when too high (**8**, 10 kDa, 40% and **9**, 400−1000 kDa, 20%), solubility was impaired and hence penetration as well. After a 7 h exposure, **7** (10 kDa, 20%) was localized at some spots in the SC (Figure S9), whereas **10** (400−1000 kDa, 5%) was not detected (not shown). After a 24 h exposure, **7** was homogeneously

distributed in the SC and slightly in the VE (Figure 2), but was not detected in the deeper layers of the skin, whereas **10** was only located at some spots in the SC (Figure S10). The present data showed that the penetration of a cosmetic relevant compound in the skin can be efficiently probed using a SCoMPI. As expected, the penetration is highly dependent on the size of HAs, with no modification of the skin structure.

AUTHOR INFORMATION

Corresponding Author

*E-mail: clotilde.policar@ens.fr.

ORCID

Laurence Grimaud: 0000-0003-3904-1822

Clotilde Policar: 0000-0003-0255-1650

Notes

The authors declare no competing financial interest.

ACKNOWLEDGMENTS

École Normale Supérieure (ENS), CNRS (UMR7203, 8640), PSL University, and Sorbonne Université are acknowledged for their financial support. The authors wish to thank ENS for L.H.'s PhD fellowship, PSL-Inocellchem in the frame of the contract ANR-10-IDEX-0001-02-PSL, maturation project C1532 - DM1503 MeCOX (for the development of SCoMPI probes), and *Fédération pour la recherche biomédicale* FRM DEI20151234413 (funding for an IR-microscope, namely, a Cary 620 infrared microscope equipped with a 128 × 128 pixels Stingray MCT detector) for financial support. We thank Zoher Gueroui for access and help with the fluorescence microscope, the SOLEIL committee for beamtime, and members from SMIS beamline (project 20150269).

ABBREVIATIONS

HA, hyaluronic acid; SC, stratum corneum; VE, viable epidermis; MW, molecular weight; (SR)-FTIR-SM, (synchrotron radiation) Fourier transform infrared spectromicroscopy; ROI, region of interest; SCoMPI, Single core multimodal probe for imaging; DIPEA, diisopropylethylamine; TFA, trifluoroacetic acid

REFERENCES

(1) Weissmann, B., and Meyer, K. (1954) The Structure of Hyalobiuronic Acid and of Hyaluronic Acid from Umbilical Cord1,2. *J. Am. Chem. Soc. 76*, 1753−1757.

(2) Shiedlin, A., Bigelow, R., Christopher, W., Arbabi, S., Yang, L., Maier, R. V., Wainwright, N., Childs, A., and Miller, R. J. (2004) Evaluation of Hyaluronan from Different Sources: Streptococcus zooepidemicus, Rooster Comb, Bovine Vitreous, and Human Umbilical Cord. *Biomacromolecules 5*, 2122−2127.

(3) Pavicic, T., Gauglitz, G. G., Lersch, P., Schwach-Abdellaoui, K., Malle, B., Korting, H. C., and Farwick, M. (2011) Efficacy of Cream-Based Novel Formulations of Hyaluronic Acid of Different Molecular Weights in Anti-Wrinkle Treatment. *J. Drugs Dermatol. 10*, 990−1000.

(4) Kogan, G., Šoltés, L., Stern, R., and Gemeiner, P. (2006) Hyaluronic acid: a natural biopolymer with a broad range of biomedical and industrial applications. *Biotechnol. Lett. 29*, 17−25.

(5) Clède, S., Lambert, F., Sandt, C., Gueroui, Z., Refregiers, M., Plamont, M. A., Dumas, P., Vessieres, A., and Policar, C. (2012) A rhenium tris-carbonyl derivative as a single core multimodal probe for imaging (SCoMPI) combining infrared and luminescent properties. *Chem. Commun. 48*, 7729−31.

(6) Clède, S., and Policar, C. (2015) Metal-carbonyl units for vibrational and luminescence imaging: towards multimodality. *Chem. - Eur. J. 21*, 942−58.

(7) Hostachy, S., Policar, C., and Delsuc, N. (2017) Re(I) carbonyl complexes: Multimodal platforms for inorganic chemical biology. *Coord. Chem. Rev. 351*, 172−188.

(8) Fernandez-Moreira, V., Thorp-Greenwood, F. L., and Coogan, M. P. (2010) Application of d^6 transition metal complexes in fluorescence cell imaging. *Chem. Commun. 46*, 186−202.

(9) Clède, S., Lambert, F., Sandt, C., Gueroui, Z., Delsuc, N., Dumas, P., Vessières, A., and Policar, C. (2013) Synchrotron radiation FTIR detection of a metal-carbonyl tamoxifen analog. Correlation with luminescence microscopy to study its subcellular distribution. *Biotechnol. Adv. 31*, 393−395.

(10) Stephenson, G. R. (2006) Organometallic bioprobes, *Bio-organometallics—Biomolecules, labeling, medecine* (Jaouen, G., Ed.) pp 215−262, Wiley-VCH, Weinheim.

(11) Salmain, M., Vessières, A., Jaouen, G., and Butler, I. S. (1991) Fourier transform spectroscopic method for the quantitative trace analysis detection of transition-metal carbonyl-labeled bioligands. *Anal. Chem. 63*, 2323−2329.

(12) Amoroso, A. J., Arthur, R. J., Coogan, M. P., Court, J. B., Fernández-Moreira, V., Hayes, A. J., Lloyd, D., Millet, C., and Pope, S. J. A. (2008) 3-Chloromethylpyridyl bipyridine fac-tricarbonyl rhenium: a thiol-reactive luminophore for fluorescence microscopy accumulates in mitochondria. *New J. Chem. 32*, 1097.

(13) Raszeja, L. J., Siegmund, D., Cordes, A. L., Guldenhaupt, J., Gerwert, K., Hahn, S., and Metzler-Nolte, N. (2017) Asymmetric rhenium tricarbonyl complexes show superior luminescence properties in live cell imaging. *Chem. Commun. 53*, 905−908.

(14) Agorastos, N., Borsig, L., Renard, A., Antoni, P., Viola, G., Spingler, B., Kurz, P., and Alberto, R. (2007) Cell-specific and nuclear targeting with [M(CO)(3)](+) (M = (99m)Tc, Re)-based complexes conjugated to acridine orange and bombesin. *Chem. - Eur. J. 13*, 3842−52.

(15) Coogan, M. P., and Fernandez-Moreira, V. (2014) Progress with, and prospects for, metal complexes in cell imaging. *Chem. Commun. 50*, 384−399.

(16) Coogan, M. P., Doyle, R. P., Valliant, J. F., Babich, J. W., and Zubieta, J. (2014) Single amino acid chelate complexes of the $M(CO)_3^+$ core for correlating fluorescence and radioimaging studies (M = 99mTc or Re). *J. Labelled Compd. Radiopharm. 57*, 255−261.

(17) Albada, B., and Metzler-Nolte, N. (2016) Organometallic−Peptide Bioconjugates: Synthetic Strategies and Medicinal Applications. *Chem. Rev. 116*, 11797−11839.

(18) Henry, L., Schneider, C., Mutzel, B., Simpson, P. V., Nagel, C., Fucke, K., and Schatzschneider, U. (2014) Amino acid bioconjugation via iClick reaction of an oxanorbornadiene-masked alkyne with a Mn(I)(bpy)(CO)3-coordinated azide. *Chem. Commun. 50*, 15692−5.

(19) Clède, S., Delsuc, N., Laugel, C., Lambert, F., Sandt, C., Baillet-Guffroy, A., and Policar, C. (2015) An easy-to-detect nona-arginine peptide for epidermal targeting. *Chem. Commun. 51*, 2687−9.

(20) Raszeja, L., Maghnouj, A., Hahn, S., and Metzler-Nolte, N. (2011) A novel organometallic ReI complex with favourable properties for bioimaging and applicability in solid-phase peptide synthesis. *ChemBioChem 12*, 371−6.

(21) Bartholoma, M., Valliant, J., Maresca, K. P., Babich, J., and Zubieta, J. (2009) Single amino acid chelates (SAAC): a strategy for the design of technetium and rhenium radiopharmaceuticals. *Chem. Commun.*, 493−512.

(22) Gasser, G., Pinto, A., Neumann, S., Sosniak, A. M., Seitz, M., Merz, K., Heumann, R., and Metzler-Nolte, N. (2012) Synthesis, characterisation and bioimaging of a fluorescent rhenium-containing PNA bioconjugate. *Dalton Trans. 41*, 2304−2313.
(23) Santoro, G., Zlateva, T., Ruggi, A., Quaroni, L., and Zobi, F. (2015) Synthesis, characterization and cellular location of cytotoxic constitutional organometallic isomers of rhenium delivered on a cyanocobalmin scaffold. *Dalton Trans. 44*, 6999−7008.
(24) Clède, S., Lambert, F., Sandt, C., Kascakova, S., Unger, M., Harte, E., Plamont, M. A., Saint-Fort, R., Deniset-Besseau, A., Gueroui, Z., et al. (2013) Detection of an estrogen derivative in two breast cancer cell lines using a single core multimodal probe for imaging (SCoMPI) imaged by a panel of luminescent and vibrational techniques. *Analyst 138*, 5627−38.
(25) Imstepf, S., Pierroz, V., Rubbiani, R., Felber, M., Fox, T., Gasser, G., and Alberto, R. (2016) Organometallic Rhenium Complexes Divert Doxorubicin to the Mitochondria. *Angew. Chem., Int. Ed. 55*, 2792−2795.
(26) Salmain, M., and Vessières, A. (2006) Organometallic complexes as tracers in non-isotopic immunoassay, *Bioorganometallics—Biomolecules, labeling, medecine* (Jaouen, G., Ed.) pp 263−302, Wiley-VCH, Weinheim.
(27) Policar, C., Waern, J. B., Plamont, M. A., Clède, S., Mayet, C., Prazeres, R., Ortega, J.-M., Vessières, A., and Dazzi, A. (2011) Subcellular Imaging in the Mid-IR of a Metal-Carbonyl Moiety Using Photothermal Induced Resonance. *Angew. Chem., Int. Ed. 50*, 860−864.
(28) Hostachy, S., Swiecicki, J. M., Sandt, C., Delsuc, N., and Policar, C. (2016) Photophysical properties of single core multimodal probe for imaging (SCoMPI) in a membrane model and in cells. *Dalton Trans. 45*, 2791−2795.
(29) Clède, S., Lambert, F., Saint-Fort, R., Plamont, M. A., Bertrand, H., Vessieres, A., and Policar, C. (2014) Influence of the side-chain length on the cellular uptake and the cytotoxicity of rhenium triscarbonyl derivatives: a bimodal infrared and luminescence quantitative study. *Chem. - Eur. J. 20*, 8714−22.
(30) Dazzi, A., and Policar, C. (2011) AFM-IR: photothermal infrared nanospectroscopy: Application to cellular imaging, *Biointerface Characterization by Advanced IR Spectroscopy* (Pradier, C. M., and Chabal, Y. J., Ed.) pp 245−278, Elsevier, Amsterdam.
(31) Dazzi, A., and Prater, C. B. (2017) AFM-IR: Technology and Applications in Nanoscale Infrared Spectroscopy and Chemical Imaging. *Chem. Rev. 117*, 5146−5173.
(32) Joshi, T., Pierroz, V., Mari, C., Gemperle, L., Ferrari, S., and Gasser, G. (2014) A Bis(dipyridophenazine)(2-(2-pyridyl)pyrimidine-4-carboxylic acid)ruthenium(II) Complex with Anticancer Action upon Photodeprotection. *Angew. Chem., Int. Ed. 53*, 2960−2963.
(33) Kitanovic, I., Can, S., Alborzinia, H., Kitanovic, A., Pierroz, V., Leonidova, A., Pinto, A., Spingler, B., Ferrari, S., Molteni, R., et al. (2014) A Deadly Organometallic Luminescent Probe: Anticancer Activity of a ReI Bisquinoline Complex. *Chem. - Eur. J. 20*, 2496−2507.
(34) Fudala, R., Mummert, M. E., Gryczynski, Z., and Gryczynski, I. (2011) Fluorescence detection of hyaluronidase. *J. Photochem. Photobiol., B 104*, 473−477.
(35) El Kaim, L., and Grimaud, L. (2009) Beyond the Ugi reaction: less conventional interactions between isocyanides and iminium species. *Tetrahedron 65*, 2153−2171.
(36) Cheron, N., Ramozzi, R., El Kaim, L., Grimaud, L., and Fleurat-Lessard, P. (2012) Challenging 50 years of established views on Ugi reaction: a theoretical approach. *J. Org. Chem. 77*, 1361−6.
(37) Creaser, C. S., Fey, M. A., and Stephenson, G. R. (1994) Environment sensitivity of IR-active metal carbonyl probe groups. *Spectrochim. Acta, Part A 50*, 1295−1299.
(38) Fernández, E., Rodríguez, G., Hostachy, S., Clède, S., Cócera, M., Sandt, C., Lambert, F., de la Maza, A., Policar, C., and López, O. (2015) A rhenium tris-carbonyl derivative as a model molecule for incorporation into phospholipid assemblies for skin applications. *Colloids Surf., B 131*, 102−107.
(39) Clède, S., Policar, C., and Sandt, C. (2014) Fourier transform infrared (FT-IR) spectromicroscopy to identify cell organelles: correlation with fluorescence staining in MCF-7 breast cancer cells. *Appl. Spectrosc. 68*, 113−7.
(40) Merle, C., and Baillet-Guffroy, A. (2009) Physical and chemical perturbations of the supramolecular organization of the stratum corneum lipids: In vitro to ex vivo study. *Biochim. Biophys. Acta, Biomembr. 1788*, 1092−1098.
(41) Cotte, M., Dumas, P., Besnard, M., Tchoreloff, P., and Walter, P. (2004) Synchrotron FT-IR microscopic study of chemical enhancers in transdermal drug delivery: example of fatty acids. *J. Controlled Release 97*, 269−281.
(42) Mendelsohn, R., Flach, C. R., and Moore, D. J. (2006) Determination of molecular conformation and permeation in skin via IR spectroscopy, microscopy, and imaging. *Biochim. Biophys. Acta, Biomembr. 1758*, 923−933.